

PACS numbers: 42.65.Dr;42.62.Fi;33.20.Sn
DOI: 10.1070/QE2005v035n02ABEH002896

Transient CARS spectroscopy of rotational transitions in H_2: the statistical dependences of the Doppler and collision dephasing

V.G. Arakcheev, A.A. Valeev, V.B. Morozov, A.N. Olenin, V.G. Tunkin, D.V. Yakovlev

***Abstract*. The $S_0(0)$ and $S_0(1)$ rotational transitions in the H_2 molecules are studied by the method of transient CARS spectroscopy at temperatures 296 and 80 K in a broad range of gas densities – from the density at which Doppler dephasing occurs to the density corresponding to collision dephasing. The slowest decay of the responses of the scattered probe pulse at the molar gas density ~ 0.2 amagat corresponds to the Dicke line narrowing. It is shown that the dephasing of the $S_0(1)$ transition in the natural H_2 mixture leads to a substantial discrepancy between the experimental results and the model of statistically independent perturbations of the rotational and translational motion of molecules at densities within a few tenths of amagat. This discrepancy becomes quite significant at liquid nitrogen temperature. At the same time, the dephasing of the $S_0(0)$ transition better corresponds to this model, as well as the dephasing of the $S_0(1)$ transition in the buffer He gas. The deviation from the model of statistically independent perturbations is described by introducing the correlation parameter. It is assumed that the features of the dephasing of the $S_0(1)$ transition observed in the natural H_2 mixture are mainly caused by resonance dephasing collisions.**

Keywords: *H_2 molecule, transient CARS spectroscopy, collision dephasing, Dicke effect, resonance interaction.*

1. Introduction

Dephasing of the H_2 molecule transitions is of interest for understanding the fundamental aspects of intermolecular interactions and also for developing methods for hydrogen diagnostics. The purely rotational transitions in H_2 have been studied in many papers, in particular, [1 – 6] by the method of spontaneous Raman scattering. The influence of collisions on the broadening and shift of vibrational – rotational resonances of hydrogen molecules has been investigated by the methods of coherent anti-Stokes Raman scattering (CARS) [7, 8], stimulated Raman amplification, and inverse Raman scattering [9]. The transient variant of CARS, featuring the properties of high-resolution spectroscopy [10, 11], can be efficiently used for studying inhomogeneously broadened resonances of H_2 [12 – 14]. Under the simultaneous action of several dephasing mechanisms, it is important to consider correctly their mutual influence and correlations.

The statistical dependence of collision perturbations of the translational and vibrational (rotational) motions of molecules was discussed in several theoretical papers [15 – 18]. Rautian and Sobel'man showed [17] that these two types of perturbations should be considered together because the phase of vibrations (rotations) and the translational velocity of molecules can change during the same collision; moreover, variations in the phase and velocity can be interrelated. One should expect that correlations between the perturbations of the phase and velocity can be most distinct at gas densities at which these perturbations make comparable contributions to the line broadening. It is at such densities that the Dicke effect can be observed.

The Dicke narrowing for the $S_0(1)$ rotational transition in hydrogen was observed in several papers by the method of spontaneous Raman scattering, but only in the case of perpendicular scattering geometry [1 – 4]. Irrespective of the scattering geometry, the spectral width (FWHM) $\Delta\nu$ of the line in the model of statistically independent phase and velocity perturbations in the density range where the Dicke narrowing is observed is described by the expression [19]

$$\Delta\nu = \frac{k^2 D_0}{\pi\rho} + \gamma\rho, \tag{1}$$

where $k = |\boldsymbol{k}_1 - \boldsymbol{k}_s|$; $\boldsymbol{k}_1$ and $\boldsymbol{k}_s$ are the wave vectors of the pump and scattered waves, respectively; ρ is the gas density in amagat (1 amagat under normal conditions corresponds to the molar volume 22.414 m^3 $kmol^{-1}$ or the concentration of particles 2.68×10^{19} cm^{-3}); D_0 is the diffusion coefficient for $\rho = 1$ amagat; and γ is the broadening coefficient.

For the 587-cm^{-1} $S_0(1)$ rotational transition in the H_2 molecule pumped by a 632.8-nm He – Ne laser in the case of the perpendicular scattering geometry, we have $k/2\pi = 21.9 \times 10^3$ cm^{-1}. By taking the broadening coefficient $\gamma = 3.3 \times 10^{-3}$ cm^{-1} $amagat^{-1}$ [20] and the diffusion coefficient $D_0 = 1.34$ cm^2 amagat s^{-1}[21], we estimate the density $\rho_{min} = [k^2 D_0/(\pi\gamma)]^{1/2}$ amagat at which $\Delta\nu$ achieves the minimum value $\Delta\nu_{min} = 2k(\gamma D_0/\pi) = 2\gamma\rho_{min}$: $\rho_{min} =$ 9 amagat, in this case $\Delta\nu_{min} = 0.06$ cm^{-1} (at temperature $T = 296$ K). It is at the density ~ 9 amagat that the Dicke narrowing was observed for the $S_0(1)$ transition [1 – 4]. In some of these papers, the minimum width of the transition was found to be larger than $\Delta\nu_{min}$. The agreement between the experiment and the model of statistically independent

V.G. Arakcheev, A.A. Valeev, V.B. Morozov, A.N. Olenin, V.G. Tunkin, D.V. Yakovlev International Teaching and Research Laser Center, M.V. Lomonosov Moscow State University, Vorob'evy gory, 119992 Moscow, Russia

Received 30 September 2004; revision received 17 December 2004
Kvantovaya Elektronika **35** (2) 128 – 134 (2005)
Translated by M.N. Sapozhnikov

perturbations of translational and rotational molecular motions was achieved in papers [1, 3, 4], where the so-called optical diffusion coefficient ($1.6-1.8$ cm^2 amagat s^{-1}), which exceeds the diffusion coefficient, was used. The authors of these papers claimed that this fact is the experimental proof of the presence of correlation.

For the collinear geometry of forward scattering corresponding to coherent scattering, we have $k/2\pi = 587$ cm^{-1} and in this case $\rho_{\min} = 0.25$ amagat, and $\Delta\nu_{\min} = 1.5 \times 10^{-3}$ cm^{-1} (at 296 K). It is preferable to begin measurements at lower densities, when Doppler dephasing dominates ($\rho < 0.01$ amagat). Therefore, the method of coherent Raman scattering spectroscopy should have both a sufficiently high spectral resolution and rather high sensitivity. The width of the $S_0(1)$ line of hydrogen as a function of ρ was measured with a spectral resolution of 10^{-4} cm^{-1} by using stimulated Raman amplification [20]; however, these measurements were performed for $\rho \geqslant 1$ amagat, i.e., above densities at which the Dicke effect is observed. The sensitivity of our transient CARS spectrometer allowed not only the detection of coherent scattering on the $S_0(1)$ rotational transition of the H_2 molecule at the gas density of 0.006 amagat (at 296 K) but also the detection of the signal decay at this density within the dynamic range of no less than three orders of magnitude.

In this paper, we used the method of transient CARS spectroscopy to study the $S_0(0)$ and $S_0(1)$ rotational transitions of the H_2 molecule in a broad range of gas densities – from the density at which Doppler dephasing is observed to the density corresponding to collision dephasing. We investigated the natural H_2 mixture (nH_2) at room (296 K) and liquid nitrogen temperatures. At room temperature, H_2 was also used in the He buffer gas. A special attention was devoted to the densities at which the Dicke effect is observed and deviations from the model of statistically independent perturbations are most likely.

2. Theoretical model

2.1 Pulsed response

A pulsed response measured in the experiment as a result of scattering a probe pulse with the amplitude $A_p(t)$ and delay time τ is calculated from the expression [18]

$$W(\tau) = \int_0^\infty |A_p(t)Q(t+\tau)|^2 \mathrm{d}t, \tag{2}$$

where

$$Q(t) = \int_0^\infty A(t-t')H(t')\mathrm{d}t \tag{3}$$

is the coherence induced by a biharmonic pump with the amplitude $A(t) = A_1(t)A_2(t)$ [$A_1(t)$ and $A_2(t)$ are the amplitudes of the pump waves]; $H(t)$ is the Green function representing the response of the system to the δ perturbation. If the duration of the pump and probe pulses can be neglected compared to the characteristic time of signal variation, we obtain

$$W(\tau) \sim |H(\tau)|^2. \tag{4}$$

In the case of purely rotational transitions in H_2 molecules, dephasing is determined by the Doppler effect, whose contribution is modified taking into account collisions changing the magnitude and direction of the velocity of molecules, and by the perturbations of the phase of the rotational motion of molecules in collisions (collision dephasing).

2.2 Statistical independence

In the model of statistically independent perturbations, the Green function $H(t)$ is defined as the product of the components describing the Doppler [$H_D(t)$] and collision [$H_c(t)$] dephasings:

$$H(t) = H_D(t)H_c(t), \tag{5}$$

where $H_D(t)$ has the form [21]

$$H_D(t) = \exp[-L(t)]; \quad L(t) = k_0^2\sigma_V^2 \int_0^t (t-t')R(t')\mathrm{d}t'; \tag{6}$$

$\sigma_V^2 = kT/M$ is the dispersion of the velocity distribution of molecules; M is the molecular mass; $\sigma_V^2 R(t)$ is the correlation function of the velocity; $k_0 = \omega_0/c$; and $\omega_0/(2\pi c) = 587$ cm^{-1}. Irrespective of the form of the correlation coefficient $R(t)$, we obtain

$$L(t) = \begin{cases} k_0^2\sigma_V^2 t^2/2 & \text{for } t \ll \tau_V, \\ k_0^2 D(t-\tau_0) & \text{for } t \gg \tau_V, \end{cases}$$

where τ_V is the velocity correlation time; $D = \sigma_V^2 \int_0^\infty R(t)\mathrm{d}t = \sigma_V^2\tau_V$ is the diffusion coefficient; and $\tau_0 = \tau_V^{-1}\int_0^\infty tR(t)\mathrm{d}t$.

In the model of weak collisions, in which the correlation coefficient has the form $R(t) = \exp(-|t|/\tau_V)$ [18], the Doppler part of the Green function is

$$H_V(t) = \exp\{-k_0^2\tau_V^2\sigma_V^2[t/\tau_V - 1 + \exp(-t/\tau_V)]\}. \tag{7}$$

In the case of strong collisions, when the correlation coefficient can be taken from [10] in the form $R(t) = (1+t^2/\tau_V^2)$, we obtain

$$H_V(t) = \exp\{-k_0^2\tau_V^2\sigma_V^2[(1+t^2/\tau_V^2)^{1/2} - 1]\}. \tag{8}$$

Depending on the relation between t and τ_V, the function H_V transforms from a Gaussian [$(\exp(-k_0^2\sigma_V^2 t^2/2)$ for $t \ll \tau_V$] to a Lorentzian [$\exp(-k_0^2\sigma_V^2 t/\tau_V)$ for $t \gg \tau_V$]. In semilogarithmic coordinates, this looks like a gradual straightening and rise of the pulsed response curve with increasing density. For $\tau_V \to 0$, the Doppler part of the Green function degenerates to a horizontal straight line $H_V(t) = 1$. In this case, the Doppler contour experiences a collapse.

Assuming that the collision duration is small compared to the delay time, the collision dephasing is described by the exponential

$$H_c(t) = \exp(-t/T_2). \tag{9}$$

Within the framework of our model, the time parameters T_2 and τ_V are inversely proportional to ρ: $T_2 = T_{20}/\rho$, $\tau_V = D/\sigma_V^2 = D_0/(\rho\sigma_V^2)$, where T_{20} is the dephasing time. The shape of the spectral line determined by dephasing

caused by statistically independent perturbations of translational (in the model of weak collisions) and rotational (vibrational) motions is known as the Galatry contour [22, 23].

2.3 Consideration of the statistical dependence

In [15], a model is considered which takes into account the statistical dependence of the collision perturbations of the translational and vibrational (rotational) motions of a molecule. The correlation function was described by the expression

$$\Phi(\tau) = \exp\left[-\Gamma\tau - \frac{\Delta\omega_D^2}{2\tilde{\nu}_d^2}(\tilde{\nu}_d\tau - 1 + e^{-\tilde{\nu}_d\tau})\right], \qquad \tilde{\nu}_d \equiv \nu_d\left(1 - \frac{\Gamma}{\nu}\right), \tag{10}$$

where $\Gamma = \rho/T_{20}$; $\nu_d = kT/(MD)$; and ν is a parameter of the model. Because $\nu_d > \tilde{\nu}_d$, we can conclude that the statistical dependence taken into account in (10) reflects the weakening of the collapse of the Doppler contour caused by the fact that in the same collisions, along with changes in the magnitude and direction of the velocity, the irreversible phase interruption also occurs. Because transient spectroscopy deals with time-resolved measurements and $\tau_V = 1/\nu_d$, we will take the statistical dependence into account similarly to (10) in the following way

$$H_V(t) = \exp\{-k_0^2\tilde{\tau}_V^2\sigma_V^2[\tau/\tilde{\tau}_V - 1 + \exp(-t/\tilde{\tau}_V)]\}, \qquad \tilde{\tau}_V = \tau_V\left(1 + \alpha\frac{\rho}{T_{20}}\right), \tag{11}$$

where α is the correlation degree.

3. Experiment

3.1 Experimental setup

We used the experimental setup that was similar to that described in [14]. A passively mode-locked Nd : YAG oscillator with a negative feedback emitted a train of ten 30-ps pulses. A separated single central pulse was amplified and converted to the second harmonic at 0.532 μm. The 354-cm^{-1} $S_0(0)$ and 587-cm^{-1} $S_0(1)$ transitions were excited by biharmonic pumping using the 0.532-μm second harmonic pulse from a master Nd : YAG oscillator and the amplified pulse (0.542 and 0.549 μm) from a dye laser. The probe pulse was the 0.355-μm third harmonic pulse from the master oscillator. The probe pulse was delayed with respect to pump pulses with the help of a four-pass scanned corner-reflector delay line. The pump and probe beams were focused by a lens with the focal length $F = 100$ cm to the centre of a 100-cm cell containing either nH_2 or a mixture of 10 % of H_2 with the buffer helium gas.

The purity of H_2 used in experiments was 99.99 %. The gas pressure was measured with a vacuum gauge. Taking into account the error of pressure measurements and variations in room temperature within ±2°, the error of density measurements was ±2.5 % for $0.06 < \rho < 1$ amagat and increased with decreasing density up to ±6 % for $\rho =$ 0.01 amagat.

In experiments with nH_2 cooled to liquid nitrogen temperature, we used a low-temperature 25-cm cell having a jacket with liquid nitrogen and a vacuum case [14]. The pump and probe beams were focused by a lens with the focal length 30 cm to the centre of the cell. The temperature in the cell was controlled with a thermocouple attached to its side wall. The difference of temperatures in the cell and in a Dewar with liquid nitrogen (73 K) was measure to be 7 K, i.e., the temperature in the cell was about of 80 K.

The overlap of the pump and probe beams was controlled with a CCD camera. The pump pulse energy was reduced to the level excluding the generation of high-order Raman components. The anti-Stokes signal was separated with a double monochromator. The dependence of the anti-Stokes pulse energy W_a on the delay time τ was recorded using a photomultiplier.

The measurements should be performed taking into account the distortions of the pulsed response, which can appear due to some misalignment of the interacting beams during the delay line scanning. The correction was performed by the results of measurement of the pulsed response, which depended only on temperature, i.e., in the Doppler regime. At room temperature, the responses for the $S_0(1)$ and $S_0(0)$ transitions completely coincide during 10 ns and cannot be used for the correction over the entire range of delay times. The Doppler response of the $S_0(0)$ transition in a cell cooled by liquid nitrogen down to 80 K has the slowest decay, which can be measured up to the largest time delays, i.e., up to 16.5 ns. It is this response that was used to determine the required correction (Fig. 1). For this purpose, we drew a smoothed curve through the experimental points, which was compared with the theoretical Doppler response at 80 K. The error was determined as the difference of these curves. All the pulsed responses measured in the experiment were corrected taking this error into account. Good agreement of the experimental Doppler responses of the $S_0(1)$ and $S_0(0)$ transitions corrected by this method with the results of calculations at 296 K (see Figs 2 and 4) confirms the validity of the method.

3.2 Experimental results

The pulsed responses $W_a(\tau)$ of the $S_0(1)$ transition measured at different hydrogen densities at 296 and 80 K and corrected by the method described above are presented in Figs 2 and 3, respectively. Each of the points in these

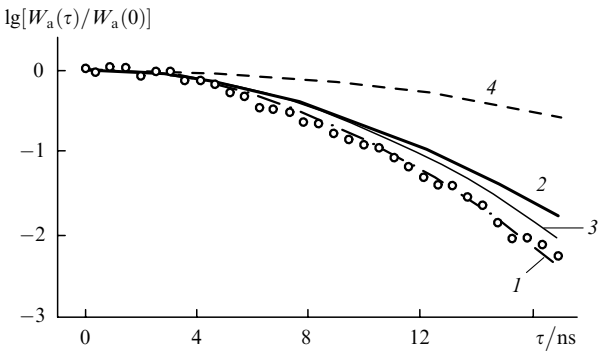

Figure 1. Method for the correction of pulsed responses: the experimental pulsed response of the $S_0(0)$ transition at 80 K and the density $\rho = 0.004$ amagat (circles); the result of fitting (*1*); the response calculated by using the model of statistically independent dephasing mechanisms (*2*); the Doppler response (*3*); the correction (*4*) determined as the difference between curves (*2*) and (*1*).

figures is the result of averaging of three series of measurements (delay line scanning cycles) over 15 laser shots for each delay time. The pulsed response curves for different densities are shifted with respect to each other along the vertical axis for convenience of the presentation. The responses $W_a(\tau)$ measured at lowest densities, 0.006 (296 K) and 0.004 amagat (80 K), are close to Gaussians, i.e., parabolic in the semilogarithmic coordinates (Doppler dephasing). At higher densities, the decay of the function $W_a(\tau)$ slows down: thus the Dicke effect appears in the temporal representation. The slowest decay is observed at 0.2–0.3 (296 K) and 0.1–0.2 amagat (80 K). At even more higher densities, the function $W_a(\tau)$ decays faster due to collision dephasing. For $\rho \geqslant 3$ amagat, the slope of the pulsed response is virtually determined only by collision dephasing, i.e., by γ. By using the response $W_a(\tau)$ measured at $\rho = 13.9$ amagat (Fig. 2), we obtained the broadening coefficient $(3.4 \pm 0.1) \times 10^{-3}$ cm^{-1} amagat^{-1} at 296 K. The dependences $W_a(\tau)$ calculated within the framework of the model of weak collisions (7) at 296 K by using $\gamma = 3.4 \times 10^{-3}$ cm^{-1} amaga^{-1} and the diffusion coefficient $D_0 = 1.34$ cm^2 amagat s^{-1} are presented in Fig. 2 by thick curves. Note that the calculation of $W_a(\tau)$ using the models of weak and strong collisions under the conditions considered in the paper gave virtually the same results, therefore, below we will use for definiteness the calculation results obtained in the model of weak collisions.

The broadening coefficient at 80 K obtained by using the response $W_a(\tau)$ measured at $\rho = 3.1$ amagat (Fig. 3) was $(3.65 \pm 0.2) \times 10^{-3}$ cm^{-1} amagat^{-1}. The diffusion coefficient $D_0 = 0.52$ cm^2 amagat s^{-1} at 80 K was found by using the diffusion coefficient $D = 0.172$ cm^2 amagat s^{-1} measured at 85 K and the pressure of hydrogen molecules

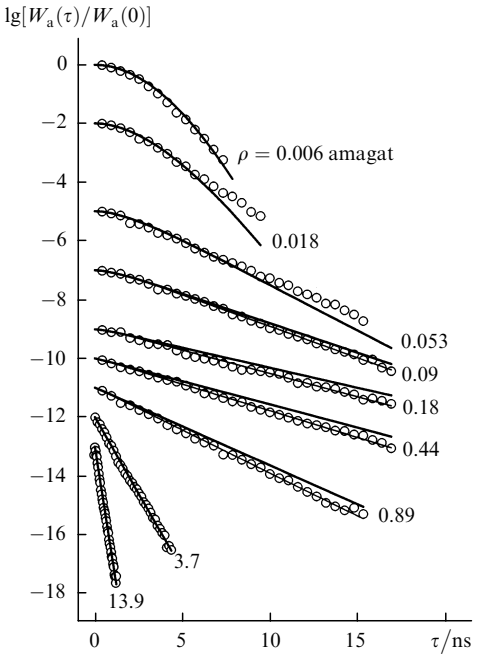

Figure 2. Experimental (circles) and theoretical (curves) pulsed responses for different ρ for the $S_0(1)$ transition at 296 K ($\gamma = 3.4 \times 10^{-3}$ cm^{-1} amagat^{-1}, $D_0 = 1.34$ cm^2 amagat s^{-1}) calculated by neglecting the correlation between velocity variations and the phase interruption in collisions (thick curves) and taking this correlation into account (thin curves).

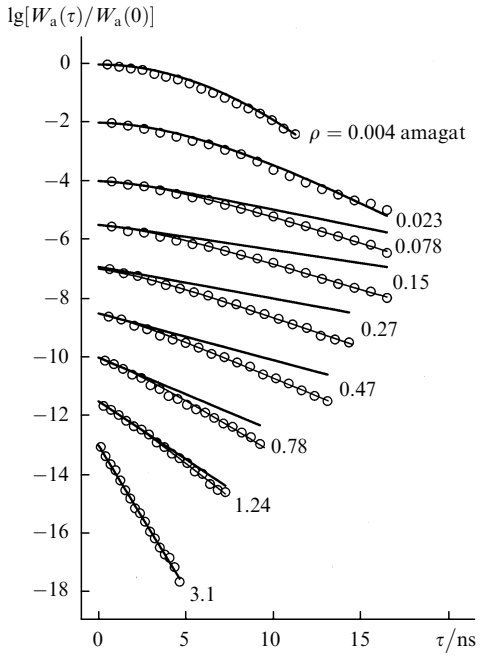

Figure 3. Experimental (circles) and theoretical (curves) pulsed responses for different ρ for the $S_0(1)$ transition at 80 K ($\gamma = 3.65 \times 10^{-3}$ cm^{-1} amagat^{-1}, $D_0 = 0.52$ cm^2 amagat s^{-1}) calculated by neglecting the correlation between velocity variations and the phase interruption in collisions (thick curves) and taking this correlation into account (thin curves).

equal to 1 atm [21]. The responses $W_a(\tau)$ calculated at 80 K by using the values of $\gamma = 3.65 \times 10^{-3}$ cm^{-1} amagat^{-1} and $D_0 = 0.52$ cm^2 amagat s^{-1} are shown in Fig. 3 by thick curves.

In the density range where the Dicke effect is observed, the discrepancy was found between the experimental results and the model of statistically independent perturbations: the experimental pulsed responses decay faster than the theoretical ones. Note that the decay rates corresponding to the weakest decays of experimental responses almost coincide at 80 and 296 K.

The pulsed responses of the $S_0(0)$ transition, measured at different densities of hydrogen at 296 and 80 K, are shown in Figs 4 and 5, respectively. The responses $W_a(\tau)$ were calculated by using the model of statistically independent perturbations with $\gamma = 3.2 \times 10^{-3}$ cm^{-1} amagat^{-1}, $D_0 = 1.34$ cm^2 amagat s^{-1} at 296 K and $\gamma = 2.45 \times 10^{-3}$ cm^{-1} $\times$amagat^{-1} (this value is lower by $\sim 5\%$ than that measured earlier [14] when the temperature was determined less accurately), $D_0 = 0.52$ cm^2 amagat s^{-1}at 80 K. One can see that the experimental pulsed responses at 80 K are well described by the model over the entire density range studied. At 296 K, the experimental pulsed responses decay somewhat faster than the calculated ones only for three densities in the region of the maximal Dicke effect.

4. Discussion of results

In the first Raman studies performed in 1968–1972 [1], the broadening coefficient γ for the $S_0(1)$ transition of the H_2 molecule was measured to be 3.7×10^{-3} cm^{-1} amagat^{-1}, while the value of γ found by the method of stimulated Raman amplification [20] was 3.3×10^{-3} cm^{-1} amagat. The value $\gamma = (3.4 \pm 0.1) \times 10^{-3}$ cm^{-1} amagat^{-1} that we obtai-

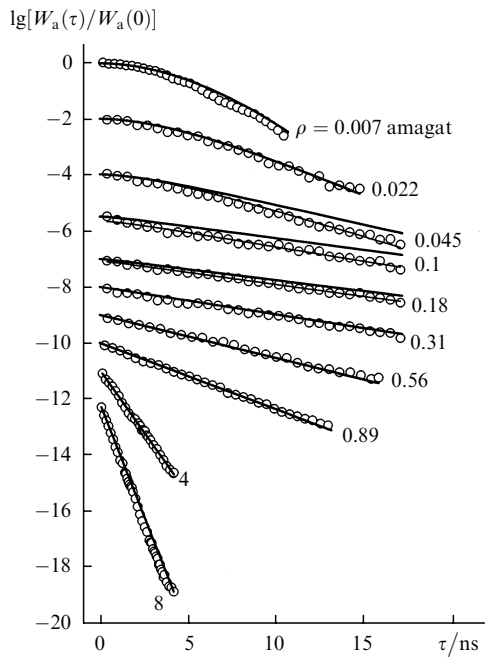

Figure 4. Experimental (circles) and theoretical (curves) pulsed responses for different ρ for the $S_0(0)$ transition at 296 K ($\gamma = 3.2 \times 10^{-3}$ cm^{-1} amagat^{-1}, $D_0 = 1.34$ cm^2 amagat s^{-1}) calculated by neglecting the correlation between velocity variations and the phase interruption in collisions (thick curves) and taking this correlation into account (thin curves).

ned at 296 K is close to the latter result. The broadening coefficient at 80 K that we measured was $(3.65 \pm 0.2) \times 10^{-3}$ cm^{-1} amagat^{-1}, which is somewhat greater than the value 3.3×10^{-3} cm^{-1} amagat^{-1} measured at 77.8 K for the $S_0(1)$ transition [24].

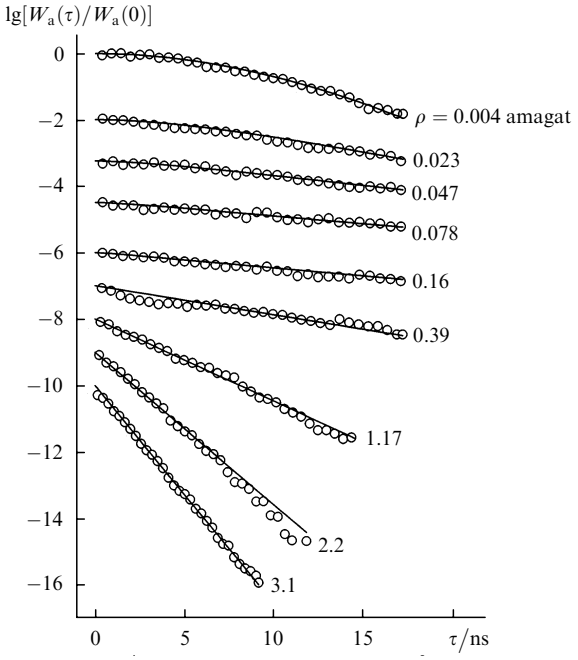

Figure 5. Experimental (circles) and theoretical (curves) pulsed responses for different ρ for the $S_0(0)$ transition at 80 K ($\gamma = 2.45 \times 10^{-3}$ cm^{-1} amagat^{-1}, $D_0 = 0.52$ cm^2 amagat s^{-1}).

The values of diffusion coefficients presented in the previous section provide good agreement between the experimental and calculated pulsed responses for densities somewhat lower than ρ_{min}, where the responses are most sensitive to the diffusion coefficient. This means that these values of D_0 are optimal for our model.

By introducing the correlation of the two dephasing mechanisms to calculations according to (11), we determined the correlation coefficient α by fitting (thin curves in Figs 2–4) for densities at which the experimental responses decay faster than the theoretical ones. One can see from Fig. 6 that the values of α for the $S_0(1)$ transition are grouped near 3 ± 1 ns (296 K) and 40 ± 15 ns (80 K). The coefficients α measured for the $S_0(0)$ transition at 296 K and $\rho \sim \rho_{min}$ have a large scatter of 15 ± 10 ns and their average value is substantially higher than that for the $S_0(1)$ transition. Note that in the case of large delay times, the two experimental responses for $\rho < \rho_{min}$ at 296 K decay slower than the calculated responses, which cannot be explained by the experimental error and corresponds to the negative correlation. However, because the experimental data are insufficient, we restrict ourselves in this case only to the statement of this fact.

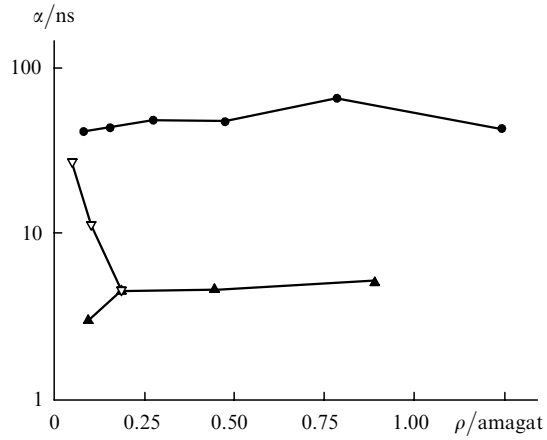

Figure 6. Dependences of the correlation coefficient α, determined by fitting experimental pulsed responses using model (11), on the density ρ for the $S_0(1)$ transition at 296 K (▲) and 80 K (○) and the $S_0(0)$ transition at 296 K (△).

As shown above, the deviation from the model of statistically independent perturbations, which is the most noticeable at 80 K, is observed for the $S_0(1)$ transition in nH_2. The natural hydrogen mixture at room temperature consists of 74.9 % of orthohydrogen (oH_2) and 25.1 % of parahydrogen (pH_2) [24]. This means that collisions occur predominantly between molecules of the same type, namely, between orthohydrogen molecules. At the same time, the pulsed response of the $S_0(1)$ transition of the H_2 molecules in He calculated for $D_0 = 1.42$ cm^2 amagat s^{-1}and $\gamma = 1.7 \times 10^{-3}$ cm^{-1} amagat^{-1} follows to the model of statistically independent perturbations (Fig. 7). The contribution to the broadening of the rotational lines of hydrogen in nH_2 is caused by elastic dephasing and inelastic quasi-resonance and resonance collisions [5], while in the He buffer gas – only by elastic collisions. The dephasing of the $S_0(0)$ transition in nH_2 is mainly determined by elastic and quasi-resonance collisions and to a much lower extent by

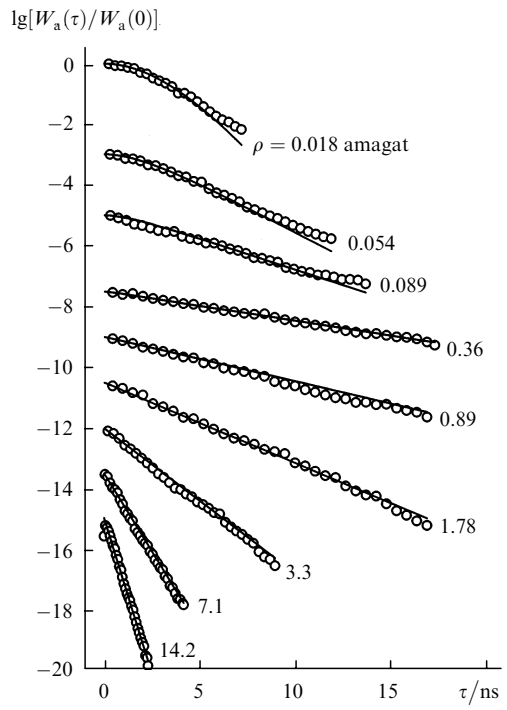

Figure 7. Experimental (circles) and theoretical (curves) pulsed responses for different ρ for the $S_0(1)$ transition at 296 K in the He buffer gas ($\gamma = 1.7 \times 10^{-3}$ cm^{-1} amagat^{-1}, $D_0 = 1.34$ cm^2 amagat s^{-1}).

resonance collisions, in which variations in the rotational energy of the two colliding molecules are completely compensated. We assume that a substantial deviation from the model of statistically independent perturbations for the $S_0(1)$ transition is related to the peculiarity of the contribution from resonance collisions.

The broadening of the rotational Raman lines of H_2 has been studied in detail in the 1970s [5, 24]. The Raman cross section σ_R (related to the broadening γ by the coefficient 7×10^{-3} cm^{-1} Å^{-2}) was measured as a function of the concentration ratio of ortho- and parahydrogen in the mixture. The opposite slopes of these functions for the $S_0(0)$ and $S_0(1)$ transitions are caused by a significant contribution of resonance collisions to the line broadening. In this case, the relative contributions of resonance collisions [determined by the broadening coefficient $\gamma_r^{(0.1)}$] to the total broadening [$\gamma_t^{(0.1)}$] are characterised by the ratio $|\sigma_{Rt}^{(0.1)}(o) - \sigma_{Rt}^{(0.1)}(p)|/\sigma_{Rt}^{(0.1)}$. The superscripts 0 and 1 correspond to the $S_0(0)$ and $S_0(1)$ transitions, respectively; and the subscripts t and r – to the total cross section (broadening) and resonance contribution, respectively; the letters o and p in parentheses correspond to the Raman cross sections for the 100 % ortho- and parahydrogen, respectively, and $\sigma_{Rt}^{(0.1)}$ is the cross section for nH_2. The studies performed in [5] allowed the separation of the partial contributions to the broadening (Raman cross section) of the transitions in oH_2 and pH_2 molecules. This permits one to calculate the broadenings (Raman cross sections) corresponding to the different types of collisions between nH_2 molecules.

At room temperature we obtain for pure hydrogen the resonance part of the cross section $\sigma_{Rr}^{(0)} = 0.093$ Å^2, $\sigma_{Rr}^{(1)} = 0.215$ Å^2 and the total Raman cross section $\sigma_{Rt}^{(0)} = 0.393$ Å^2, $\sigma_{Rt}^{(1)} = 0.483$ Å^2. The relative contribution of resonance collisions $\sigma_{Rr}^{(1)}/\sigma_{Rt}^{(1)} \sim 0.45$ is nearly twice as large as the relative contribution $\sigma_{Rr}^{(0)}/\sigma_{Rt}^{(0)} \sim 0.24$ for the $S_0(0)$ transition. This explains the fact that although the statistical dependence for the $S_0(0)$ transition is manifested at room temperature, it occurs within a narrower density range (see Fig. 6). A larger value of the coefficient α for the $S_0(0)$ transition than for the $S_0(1)$ transition is probably caused by different relations between τ_V and T_{20}. Spontaneous Raman studies [24] showed total Raman cross sections at liquid nitrogen temperature exceed by 20 % – 50 % Raman cross sections at room temperature. In this case, no information was obtained on the absolute value of partial dephasing cross sections, but the relative contributions of resonance collisions for the $S_0(0)$ and $S_0(1)$ transitions can be estimated from the value $|\sigma_{Rt}^{(0.1)}(o) - \sigma_{Rt}^{(0.1)}(p)|/\sigma_{Rt}^{(0.1)}$ (see Fig. 15 in [24]). Such an estimate gives $\sigma_{Rr}^{(0)}/\sigma_{Rt}^{(0)} \sim 0.3$ and $\sigma_{Rr}^{(1)}/\sigma_{Rt}^{(1)} \geqslant 0.9$. A substantial increase in the relative contribution of resonance collisions for the $S_0(1)$ transition is caused at least by two circumstances. First, the probability of transitions caused by the energy defect decreases with decreasing temperature, thereby reducing the role of quasi-resonance collisions in which the energies of the initial and final states are not completely compensated. Second, while at 296 K the partial fraction of molecules with $J = 3$ in nH_2, which do not contribute to the resonance collisions of molecules of a coherent ensemble, is about of 9 %, at 80 K this fraction is virtually zero. Therefore, we can conclude that the deviation from the model of statistically independent perturbations increases with increasing the relative contribution of resonance collisions.

5. Conclusions

We have shown that the dephasing of the $S_0(1)$ transition in nH_2 leads to a substantial discrepancy between experimental results and the model of statistically independent perturbations of the rotational and translational motions of molecules for the gas densities from 0.1 to ~ 1 amagat, which increases at liquid nitrogen temperature. At the same time, the dephasing of the $S_0(0)$ transition is well described by the model (except the region near the maximum manifestation of the Dicke effect at 296 K). The dephasing of the $S_0(1)$ transition in the H_2 molecule in the He buffer gas, where resonance collisions are completely absent, is well described by the model of statistically independent perturbations. The consideration of the statistical dependence of the Doppler and collision mechanisms in the dephasing model provides the agreement with the experimental results. It is assumed that the deviation from the model of statistically independent perturbations can be caused by resonance collisions, which are more efficient for the $S_0(1)$ transition in nH_2, especially at liquid nitrogen temperature.

Acknowledgements. The authors thank V.T. Platonenko for his help in the studies and A.P. Kouzov for useful discussions. This work was supported by the Russian Foundation for Basic Research (Grant No. 04-02-17282) and the International Teaching and Research Center 'Fundamental Optics and Spectroscopy'.

References

1. Cooper V.G., May A.D., Hara E.H., Knapp H.F.P. *Can. J. Phys.*, **46**, 2019 (1968).
2. Cooper V.G., May A.D., Gupta B.K. *Can. J. Phys.*, **48**, 725 (1970).
3. Gupta B.K., Hess S., May A.D. *Can. J. Phys.*, **50**, 778 (1972).
4. Gupta B.K., May A.D. *Can. J. Phys.*, **50**, 1747 (1972).
5. Keijser R.A.J., Lombardi J.R., van den Hout K.D., Sanctuary B.C., Knaap H.F.P. *Physica*, **76**, 585 (1974).
6. Edwards H.G.M., Long D.A., Sherwood G. *J. Raman Spectrosc.*, **22**, 607 (1991).
7. Farrow R.L., Zitz G.O. *J. Opt. Soc. Am. B*, **6**, 865 (1989).
8. Rahn L.A., Rosasco G.J. *Phys. Rev. A*, **41**, 3698 (1990).
9. Forsman J.W., Sinclair P.M., Duggan P., Drummond R.J. *Can. J. Phys.*, **69**, 558 (1991).
10. D'yakov Yu.E., Krikunov S.A., Magnitskii S.A., Nikitin S.Yu., Tunkin V.G. *Zh. Eksp. Teor. Fiz.*, **84**, 2013 (1983).
11. Kuznetsov D.S., Morozov V.B., Olenin A.N., Tunkin V.G. *Chem. Phys.*, **257**, 117 (2000).
12. Lang T., Kompa K.L., Motzkus M. *Chem. Phys. Lett.*, **310**, 65 (1999).
13. Lang T., Motzkus M. *J. Raman Spectrosc.*, **31**, 65 (2000).
14. Arakcheev V., Jakovlev D., Mochalov S., Morozov V., Olenin A., Tunkin V. *J. Raman Spectrosc.*, **33**, 884 (2002).
15. Rautian S.G., Sobel'man I.I. *Usp. Fiz. Nauk*, **90**, 209 (1966).
16. Gersten J.L., Foley H.M. *J. Opt. Soc. Am.*, **58**, 933 (1968).
17. Ward J., Cooper J., Smith E.W. *J. Quant. Spectr. Rad. Trans.*, **14**, 555 (1974).
18. Hess S. *Zs. Natürf.*, **25a**, 350 (1970).
19. Cherlow J.M., Porto S.P.S., in *Laser Spectroscopy of Atoms Molecules*. Ed by H. Walther (Berlin: Springer, 1976).
20. Le Flohic M.P., Duggan P., Sinclair P.M., Drummond J.R., May A.D. *Can. J. Phys.*, **72**, 186 (1994).
21. Harteck P., Schmidt H.W. *Zs. Phys. Chemie*, **21B**, 447 (1933).
22. Galatry L. *Phys. Rev.*, **122**, 1218 (1961).
23. Varghese P.L., Hanson R.K. *Appl. Opt.*, **23**, 2376 (1984).
24. Van den Hout K.D., Hermans P.W., Mazur E., Knaap H.F.P. *Physica A*, **104**, 509 (1980).